Since January 2020 Elsevier has created a COVID-19 resource centre with free information in English and Mandarin on the novel coronavirus COVID-19. The COVID-19 resource centre is hosted on Elsevier Connect, the company's public news and information website.

Transportation Research Part D 87 (2020) 102527

Contents lists available at ScienceDirect

Transportation Research Part D

journal homepage: www.elsevier.com/locate/trd

Real-time identification of aircraft sound events

Ran Giladi

School of Electrical and Computer Engineering, Ben-Gurion University, Israel

ARTICLE INFO

Keywords:
Aeroacoustics
Aircraft noise
Airport noise monitoring
Noise measurement
Noise events
Take-off
Flight path
ADS-B

ABSTRACT

Metropolitan airports constitute an environmental nuisance, mainly due to noise pollution originating from aircraft landings and takeoffs, affecting the wellbeing of the airports' neighboring populations. Noise measurement is considered the fundamental means to evaluate, enforce, validate, and control noise abatement. Noise measurements performed by sound monitors located close to urban airports are often disrupted by urban background noise that interferes with aircraft sounds. Detecting aircraft noise, classifying, identifying, and separating it from the residual background noise is a challenge for unattended aircraft noise monitors. This paper suggests a simple and inexpensive methodology, based on ADS-B (Automatic Dependent Surveillance-Broadcast), which can facilitate isolating aircraft noise from background noise. Experiments showed that using ADS-B driven noise monitors is at least as accurate as the commonly used radar–driven noise monitors, in terms of true positive, false positive, or false negative detection during the examined periods.

1. Introduction

Aircraft noise near airports located close to metropolitan areas is a long-standing environmental problem that affects the wellbeing, health, and quality of life of neighboring populations (Asensio et al., 2010;Rodríguez-Díaz et al., 2017;Sánchez-Pérez et al., 2014;Tarabini et al., 2014; Torija and Self, 2018). Aircraft noise, beyond being a matter of annoyance, contributes to the increasing incidence of a variety of health issues (e.g., sleep disturbances, cardiovascular and psychological effects, to name few) (CAA-UK, 2016). Some argue that noise pollution deteriorates the relationship between the aviation industry and neighboring communities, and may jeopardize the sustainability of this industry (Torija and Self, 2018).

This environmental issue is not new and is not expected to fade away. It became a critical issue decades ago, affecting communities and the aviation industry. The aviation industry is crucial to the economy (Zhang and Graham, 2020) and is projected to continue its annual growth rate of 4% (excluding 2020/1 due to the COVID-19 pandemic) in the coming future (ICAO, 2018). Since airports are key components of the aviation industry infrastructure, noise from aircraft takeoffs or landings in airports will increase this adverse environmental issue for nearby communities.

Various technologies, legislations, procedures, and methodologies were considered and implemented to various degrees, in an attempt to bridge between the interests of all stakeholders (EU Directive 2002/30; EU Regulation 598/2014; ICAO, 2008; ICAO, 2017; Rodríguez-Díaz et al., 2017; Tarabini et al., 2014; USC ANCA, 1990). Although technological improvements considerably reduce engine noise, aircraft airframe is still a major source of noise (mainly during landings) (Merino-Martinez et al., 2016a). The noise annoyance, from landings and takeoffs, is not expected to diminish, due to the overall air traffic growth.

Monitoring of aircraft noise is a common approach utilized by most technologies, legislations, procedures, and methodologies involved with airport sound abatement. Environmental noise measurements are applied in the design, control, enforcement, and validation of models or other noise calculations, among other activities related to noise abatement. Even in noise modeling, for example, noise measurements are required, not just to validate these models, but because compound factors change the noise created by a given aircraft type, at a certain situation and flight phase, while executing the same flight procedures. These noise variations are

https://doi.org/10.1016/j.trd.2020.102527

Available online 10 September 2020
1361-9209/

due to changing atmospheric conditions, fluctuations in the emitted noise, different operational settings, changed configurations, diverse pilots' practices and procedures, or specific adjustments (Merino-Martinez et al., 2019; Snellen et al., 2017; Zellmann et al., 2017). Noise measurements confirmed that such variations can be responsible for differences of as much as 12 dB (Gagliardi et al., 2018; Merino-Martinez et al., 2016b).

Noise measurements are therefore an indispensable tool in noise abatement efforts, for environmental protection, for communities and aviation industry sake (Asensio et al., 2012; Rodríguez-Díaz et al., 2017). However, due to background urban noise, identifying and discriminating airports' noise in residential areas close to airports is challenging (Asensio et al., 2010; Tarabini et al., 2014). Noise measurements are used to control the population's exposure to aircraft noise in residential areas, therefore the sound level meters are concurrently exposed to significant background urban noise, which interferes with the measurements (Maijala et al., 2018; Rodríguez-Díaz et al., 2017). Moreover, the ongoing reduction in engine noise complicates the problem of separating aircraft from background noise.

The International Organization for Standardization (ISO) defined and created an international standard, ISO 20906, *Acoustics - Unattended monitoring of aircraft sound in the vicinity of airports* (ISO, 2009). This standard defines the requirements for detection, classification, and identification of an aircraft sound event. It includes correlations between the noise duration and the distance between aircraft and the microphone, relation between maximum sound pressure level and the sound exposure level, spectral information, correlation of the sound event with other noise sources at known locations, and correlation with information on aircraft operations and position. To meet the challenge of background noise, the standard suggests that measurements should be performed at sites where a 15 dB gap exists between the maximum expected sound level pressure of aircraft noise events and the average residual sound (the total sound remaining after suppressing aircraft sounds).

The issue of aircraft noise measurement, and specifically separating aircraft from background noise, was dealt with by studies in the research literature, and practical solutions were offered and implemented (Rodríguez-Díaz et al., 2017).

The most common methodology for separating aircraft noise from background noise is the tracing methodology, based on synchronization of sound level measurements with the airport's surveillance radar (Asensio et al., 2010). These radars provide tracks, locations, and events of relevant aircraft noise, and trigger sound monitors to record and analyze just the relevant aircraft noise. This is a simple and accurate methodology (Asensio et al., 2012) that can be applied either in real-time or off-line (Merino-Martinez et al., 2019). However, it can only be applied by airport authorities, or subject to their consent in providing the radar tracings data. It should be noted, however, that aircraft noise misclassification still occurs, even when using radar traces (Fidell and Schomer, 2007).

Another group of techniques is based on the directivity methodology, i.e., on spatial–temporal information extracted from multiple microphones or microphone arrays. The idea is that the direction from source to the receiver is a function of the time (or phase) difference of the third-octave band power level at each microphone location. In other words, this methodology applies frequency domain beamforming to the spatial cross-correlated microphones. Examples of this methodology include identifying taxiing aircraft (Asensio et al., 2007), thrust reversing (Asensio et al., 2015), and aircraft takeoffs, landings, or fly–over (Genescà et al., 2009; Genescà et al., 2010; Merino-Martínez et al., 2020; Merino-Martinez et al., 2016b; Sánchez-Pérez et al., 2014; Snellen et al., 2017). This technique has the advantage of isolating aircraft noise from ground reflections, or ground-borne noise sources (Genescà, 2016), which represent most of the unwanted background noise source for aircraft noise measurements, and therefore microphone arrays are useful tools for that purpose. Nevertheless, it requires a rather complicated and physically large microphone setup.

Pattern recognition techniques (Asensio et al., 2010) are based on neural networks and deep learning techniques, hidden Markov models, and source separation, to name a few. They are sometimes integrated with the directivity methodology and use multi microphones (Tarabini et al., 2014). These techniques are sensitive to noisy environments, i.e., small gaps between aircraft and background noise. Examples of this methodology include identifying thrust reversing (Asensio et al., 2015), takeoff noise (Sánchez-Pérez et al., 2013), and aircraft takeoffs, landings, or fly-over (Pak and Kim, 2019; Tarabini et al., 2014). An aircraft noise likeness (ANL) methodology, based on fuzzy sets and Bayesian comparison, managed to discriminate aircraft noise from background noise, even in relatively small signal to noise ratio (SNR), i.e., more than 90% true positive for SNR $>$ 7 dB (Asensio et al., 2010). Nevertheless, there are remaining problems in the classification of aircraft noise when it is mixed with background noise (Genescà et al., 2013). The simultaneous background noise can change the noise pattern to an extent that affects the reliability of the classification, resulting in false-negative identifications.

Available techniques, based on the above-mentioned principles, are limited by cost issues, accuracy, equipment complexity, or the requirement of airport authorities' collaboration. The present paper suggests an inexpensive, accurate, simple, and independent means (other than a reliable GPS network) of separating aircraft from background noise.

The suggested methodology improves aircraft noise measurements, which are required for model validation, enforcement and control of aircraft noise abatement, and provides accurate information for the concerned population. It can be applied using a simple unattended sound monitor, or it can be used together with other discriminating techniques, such as directivity methodologies, to enhance their accuracy by triggering aircraft presence, and providing location, speed, and flight direction information.

The paper is organized as follows: the ADS-B methodology is presented in the next section, followed by a description of how to receive, record, analyze, and use ADS-B data. The experimental setup is described in section 3, and its results are reported in section 4. A conclusion section summarizes this paper.

2. The methodology

The suggested methodology of identifying aircraft noise and discriminating it from background noise is based on receiving

Automatic Dependent Surveillance-Broadcast (ADS-B) signals. These signals are transmitted practically by all aircraft relevant to the issue of airport noise, i.e., commercial passenger and cargo aircraft. Although recent research showed that nearly half of the aircraft use ADS-B (Merino-Martinez et al., 2016b), recent USA and European legislations mandate ADS-B usage during 2020, with some pushed-back deadlines (EU CIR 1207/2011; EU CIR 2020/587; US 14CFR91.225, 2019). The widespread use of ADS-B for aircraft tracking is utilized also by several applications such as Flightradar24 and FlightAware. ADS-B signals contain information about the identity of the aircraft, its location, altitude, speed, direction, and more. These signals are decoded, analyzed, and used to synchronize the aircraft's physical presence and location with the measured noise. The data obtained is equivalent to synchronizing the received noise with the airport's surveillance radar and additional information usually obtained from the airport authorities (e.g., type of plane, runway used, flight number, destination). However, the suggested method requires no cooperation from the airport authorities, which sometimes are reluctant to provide, and it certainly avoids the need for an expensive interface with the airport's data sources, primarily their surveillance radar data. Furthermore, the suggested method can be applied in areas near airports unequipped with surveillance radar at all.

ADS-B signals transmitted by aircraft enable surveillance of air-traffic instead, or in addition to, the traditional surveillance radars. Surveillance radars used in many airports for air-traffic control are basically of two types: primary and secondary surveillance radar (PSR and SSR). SSR differs from PSR in that it not only detects aircraft position but can also interrogate the aircraft by requesting information from its transponder, which thereby reply with additional information (e.g., aircraft identifier). ADS-B is an improvement of SSR, which provides additional information, regardless of SSR integrations, which is also received by other aircraft in a way that increases overall situational awareness.

ADS-B data messages are broadcast by the aircraft at approximately 0.5 s intervals, at a frequency of 1090 MHz, whereas radar signals are transmitted approximately every 4 s (ICAO, 2018a; Zhang et al., 2011). ADS-B operation depends on reliable GPS satellite systems, whereas radar operation is independent of any external resource, infrastructure, or information. ADS-B information is more accurate and more comprehensive than radar information (Zhang et al., 2011), and aircraft information can be freely acquired, decoded, and analyzed using simple and inexpensive ADS-B receivers.

As previously mentioned, most of the expensive noise measurement equipment use surveillance radars to synchronize noise and aircraft presence, to identify and discriminate aircraft from background noise. Transition to ADS-B systems as a source for synchronization is, therefore, the desired step. ADS-B is already used in several acoustics applications (Gagliardi et al., 2017; Gagliardi et al., 2018; Sánchez-Pérez et al., 2014; Snellen et al., 2017), let alone its role in air traffic control, and its reliability in the aviation industry. ADS-B dependence on GPS accuracy is tolerated, since errors are insignificant, particularly for noise synchronization (Filippone et al., 2019).

The first step in the suggested methodology is to define an enclosed corridor in the sky, through which the measured aircraft pass. A "square of interest" is defined, such that it will allow for the capture of the aircraft noise when it flies above it, at a confined altitude. Determination of the sound exposure level (SEL, LAE or $L_{p,A,e}$) requires the integration of the sound pressure level at least in the period in which the measured level is within 10dBA of L_{ASmax} (the maximum of the slow A-weighted sound pressure level) (Fig. 1). In this figure, the integration includes, for example, the two intervals marked t'_{10} and t''_{10}, but not the humps above the threshold, which are not within 10dBA of L_{ASmax}. ICAO defines this period as the "10dBA down" time (ICAO, 2015). An additional 5dBA gap is required by ISO 20,906 for reliability, separation from background noise, and the ability to measure quiet aircraft. Therefore, 15dBA is required between the background noise and L_{ASmax}.

Assuming that the sound monitor is positioned correctly according to all the ISO 20906 required specifications, the "square of interest" can be calculated. We define the shortest distance between the sound monitor and the aircraft, as shown in Fig. 2, as the *slant distance* and call it "s". Then, a distance of at least 6s should be calculated between the sound monitor and the position of the aircraft

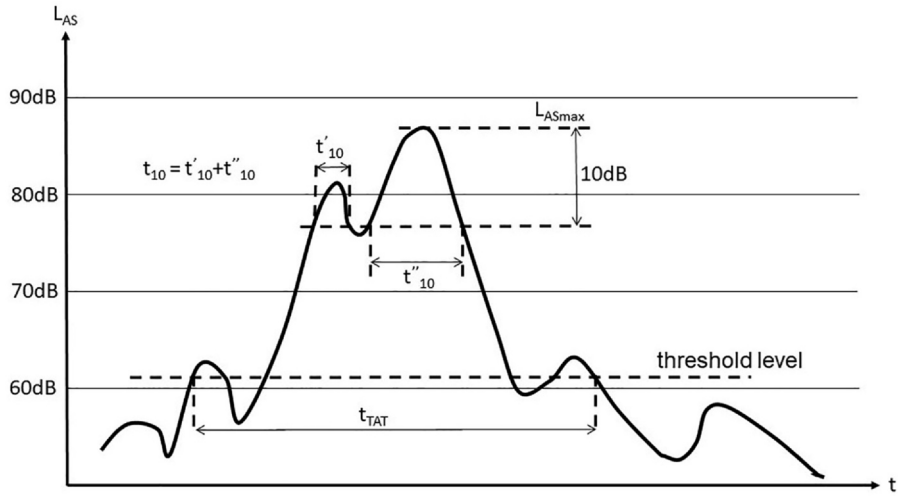

Fig. 1. Aircraft noise pattern and definitions according to ISO 20,906.

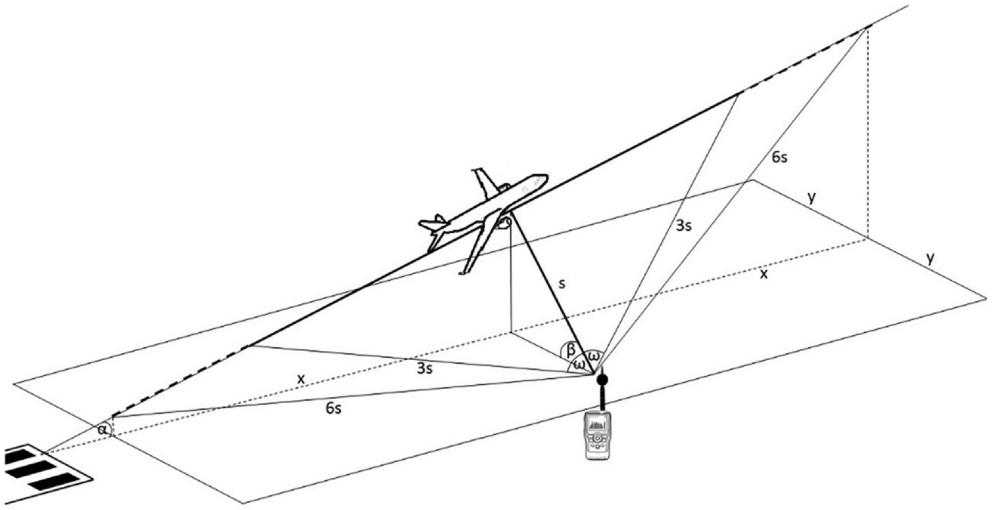

Fig. 2. Noise monitoring distances according to ISO 20906, $x \approx 6s$, $y \approx dmax$.

upon entering the "square of interest". This distance ensures a 15 dB difference in the received noise pressure level, assuming a spherical spreading of sound pressure level. The precise length of the "square of interest" is $2s\sqrt{35}\cos\alpha$, where α is the angle of climbing or descent (Fig. 2). Considering that the steepest angle of climb or descent is usually less than 20°, cos α can be ignored, and the length of the "square of interest" can be simply considered as 12s, which is a little more than the required length to receive ADS-B signals during the "10dBA down" period. The sound monitor is positioned in the midst of the length of the "square of interest". So, for example, if the sound monitor is positioned at about 400 m from the flight path and about 300 m below it, then s is about 500 m, and the length of the "square of interest" should be 6 km.

The width of the "square of interest" should be at least twice d_{max} according to ISO 20906, where d_{max} is the distance from the aircraft where the aircraft sound pressure level is 15dBA below L_{ASmax}. d_{max} can be estimated from noise-power-distance (NPD) tables associated with aircraft noise calculation programs (e.g., ECAC doc 29 (ECAC, 2016), FAA AEDT (FAA AEDT, 2017), ICAO doc 9911 (ICAO, 2018b)), or, practically, 900 m (ECAC, 2016). In condensed airports d_{max} should be narrowed as much as possible, to avoid activation of measurement by traffic originating from other runways, or, in cases of GPS disturbances or spread takeoffs (e.g., turns immediately after takeoffs) d_{max} should be widened. Such a case is demonstrated in the following (Fig. 4).

Any aircraft located above the "square of interest" at an altitude of less than 1.2 km above ground level (AGL), is a potential candidate for being detected by the measurement system.

The next step is to receive aircraft ADS-B signals. ADS-B messages contain coded aircraft identity and position (coordinates and altitude), which need to be decoded. ADS–B coded messages are publicly available and can be received and decoded by any 1090 MHz receiver (ICAO, 2012; Sun et al., 2020). When an ADS-B message is received from an aircraft that flies in the predefined enclosed corridor, it triggers the final steps, i.e., receive, record, and analyze the aircraft data simultaneously with the measured noise.

The third step is to record all the ADS-B messages from the particular aircraft that triggered the recording, along with the measured noise, starting at a noise level that is above a predefined threshold. These recordings end when the aircraft leaves the enclosed corridor, or the noise level drops below a predefined threshold for a predefined period, under ISO 20906 (ISO, 2009). The period from the beginning of a recording until its end defines the time above the threshold of that aircraft, t_{TAT}, which contains the 10-dBA down period, or t_{10}, according to ISO 20906.

The second and third steps are repeated throughout the entire monitoring period.

Processing the recorded information includes two steps: marking the time boundaries of every aircraft noise (the beginning and end of t_{TAT} or t_{10}), and estimating the aircraft position in every second of the flight during t_{TAT} or t_{10}. The latter calculation is required, since, due to various reasons (e.g., ADS-B message congestion or reception issues), not all ADS-B messages are received. The current aircraft position (at every second) is estimated based on the last received position, direction, and velocity of the aircraft in its transmitted ADS-B message. This estimation is based on polar kinematic equations, assuming no acceleration, and the resulted position is an approximation that is sufficient for the aircraft noise identification; accurate position is not required since the approximate position is enough for identifying the noise as a noise from an aircraft that is above, or close to the square of interest. Once a new ADS-B message is received, the calculations resume from this time point, according to the received position.

Processing the received noise simultaneously with the ADS-B information can be done in real-time or off-line, since the required ADS-B decoding and analysis is not complex, and can be done in milliseconds even by a simple and inexpensive computer.

3. Experimental setup

An experiment was conducted at Ben-Gurion Airport (LLBG) near Tel-Aviv, Israel. A sound monitor that identifies aircraft noise

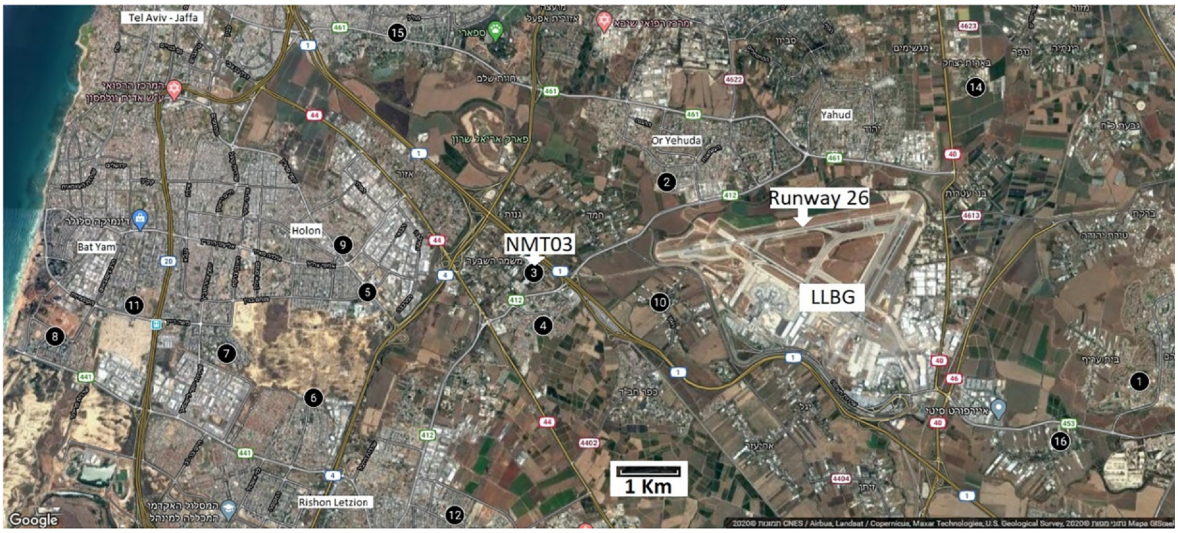

Fig. 3. Ben-Gurion airport (LLBG) and IAA's sound monitors around it. Map obtained using Google Maps.

according to the suggested methodology was compared with a monitor that is driven by the airport's surveillance radar, for identification and separation of aircraft noise.

LLBG has three runways and approximately 24 million passengers use it with about 170,000 aircraft movements a year. It is positioned amidst a metropolitan area, surrounded by towns and villages that suffer from noise pollution (Fig. 3). A network of 16 sound monitors, operated by the Israeli airport authority (IAA), encircles LLBG, which identify only about 90% of the aircraft movements, despite being connected to the airport's surveillance radar (CAA IL, 2019). Those monitors, termed NMT01 to NMT16 (i.e., Noise Monitor n), are shown in Fig. 3, taken from Google Maps, with the noise monitors' coordinates imported into a layer on the map. It should be emphasized that these sound monitors are radar-driven, i.e., the data recorded by these monitors was compared with the airport radar, and recognized as aircraft noise before storing.

Runway 26 was chosen for the experiment since it is the main takeoff runway, the busiest one, and according to the IAA, their NMT03 remote sound monitor, positioned 2 km from the end of runway 26, captures just 85.5% of aircraft takeoffs (CAA IL, 2018). This monitor is termed hereinafter "NMT03 monitor", and it is located in circle 3 in Fig. 3.

A simple ADS-B receiver was used for the current experiment, based on software-defined radio (SDR) and a Raspberry PI 3 with a TV-dongle receiver (e.g., (Taylor, 2019). A public domain program, DUMP1090 (Sanfilippo, 2012), was modified and used to capture and decode ADS–B messages in real-time. This system was coupled with an NTi XL2 sound level meter that measured and recorded the noise. This combined system (the NTi and the ADS-B receiver) is termed hereinafter "ADSB monitor", and was located at point 2 in Figure 4, 600 m away from the NMT03 monitor, located at point 1 in Fig. 4. This was the closest position to NMT03 available for placing a 24/7 noise monitor, where the distance from the flight path is about the same, and in the direction of the departing aircraft, to make sure that the NMT03 is closer to the aircraft, and should perform better. It turned out, as outline below, that both noise-monitors measured approximately the same sound levels, within the uncertainty in the measuring instrumentation.

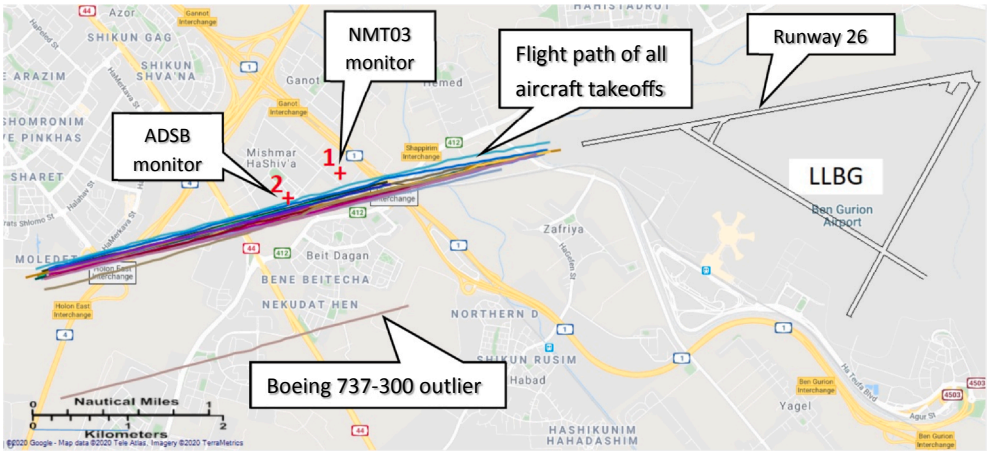

Fig. 4. Flight path of aircraft takeoffs from runway 26. Map obtained using Google Maps.

Table 1
Flight path distance from noise monitors.

	NMT03	ADSB
Aircraft average altitude (meters)	570	640
Average lateral displacement (meters)	250	100
Average slant distance (meters)	620	650

The NTi noise monitor (part of the ADSB system) recorded the received noise every second, continuously and uninterruptedly between 19.9.2019 at 12:49:22 and 23.10.2019 at 18:42:32, while the ADS-B receiver was used for specific experiments that lasted several hours, testing various algorithms and parameters.

The NMT03 system, driven by the airport radar, was supposed to work continuously during the entire experiment period, but it published aircraft noise just until 11.10.2019 at 23:54.

It is important to note that the experiment period occurred during the Israeli High Holidays month with many religious holidays, characterized by a significant traffic variance; including one day of complete cessation of activity, some days had unusually low traffic due to holidays, while others were exceptionally busy due to incoming and outgoing touristic activity. There are about 240 takeoffs from runway 26 on an average day during this period, which may vary between 350 and 150 takeoffs a day (not including the one day in which the airport was completely closed). Therefore, the ADSB system was used to examine aircraft noise identification at various traffic loads, under various background noise levels.

Since IAA's NMT03 data is published only in L_{ASmax} terms, the ADSB monitor data used for comparison was also L_{ASmax}, although L_{Aeq} was recorded along with other sound measures by the ADSB monitor.

Aircraft flight paths were recorded first by the ADSB monitor, and the "square of interest" was calculated. The aircraft average altitude at the NMT03 monitor location was 570 m, and the average horizontal distance between the NMT03 monitor and the flight paths (the lateral displacement) was 250 m. The aircraft average altitude at the ADSB monitor location was 640 m, and the average horizontal distance between the ADSB monitor location and the flight paths was 100 m. The average slant distance between the NMT03 monitor location and the aircraft was therefore 620 m, whereas it was 650 m between the ADSB monitor location and the aircraft (Table 1).

The length of the "square of interest" should, therefore, be about 8 km (12 times the slant distance), and the width should be 1800 m, as mentioned above. Fig. 4 demonstrates flight paths in the "square of interest" taken at 29.9.2019. However, flight paths of aircraft might be misplaced due to arbitrary and occasional GPS disturbance such as those occurred at that time near Ben-Gurion airport. Such an event was demonstrated in Fig. 4 by a Boeing 737–300 outlier at 10:35, that transmitted a wrong position, i.e., about 2 km south-west from its real position (which is about 1300 m aside its flight path). Such GPS disturbances required a width of 3000 m for the "square of interest", wider than the 1800 m suggested above, but small enough not to include aircraft taking off or landing from or on other runways.

Since a night curfew is imposed on takeoffs at Ben-Gurion airport from 01:40 to 05:00, five typical intervals were chosen for experiments: night (00:00–01:00), early morning (05:00–06:00), mid-day (10:00–11:00), afternoon (16:00–17:00), and evening (20:00–21:00). Additionally, experiments were separately analyzed, on a high traffic day, on a slower traffic day, and an average traffic day. Thus, the days chosen were 26/9/2019, Thursday early morning, one of the busiest periods in the airport (just before the beginning of the holiday vacations), 29/9/2019, Sunday, Holiday eve, when traffic is slow, and 24/9/2019, Tuesday, an average day.

At each of these periods, sound measurements (recorded by the ADSB monitor) that were identified as aircraft noise by the ADS-B, were compared to the measurements of the IAA's NMT03 monitor. As mentioned above, these comparisons were executed on L_{ASmax}, but this is insignificant for the experiment purpose, i.e. validating the ADS-B methodology in separating aircraft noise from residual noise.

4. Results and discussion

The NTi noise monitor (in the ADSB system) recorded noise events continuously from 19/9/2019, and the IAA published the NMT03 radar-driven aircraft noise events for the entire year of 2019. The rates of these noise and aircraft events per hour are depicted in Fig. 5, where noise events are those that were above 60dBA lasting more than 10 s (irrespective of ADS-B receiver data). It shows that 24/9/2019 is an average day in terms of traffic with more background noise events than usual, that 26/9/2019 night and early morning are busier, and that 29/9/2019 has lower traffic after early morning.

Results of 121 aircraft-noise events, taken from ten different representative time intervals as outlined above, are presented in Table 2. ADSB data contains the ADSB monitor measures, i.e., both ADS–B receiver data and the NTi noise monitor measurements. ADS–B data includes ICAO24 identity code of the detected aircraft, its position and altitude when the maximal noise (L_{ASmax}) was recorded, and the type of the aircraft according to its ICAO24 code. Noise measurements included the aircraft maximal noise (L_{ASmax}) and the time when L_{ASmax} was recorded by the ADSB monitor. The IAA data included the reported time of the aircraft takeoff, flight number, type of aircraft, and its L_{ASmax}, as reported by the NMT03 monitor.

It turns out that the L_{ASmax} measurements that were reported by the NMT03 monitor, and those reported by the ADSB monitor, were comparable (average difference of 0.6 dB, which falls within the uncertainty interval of sound measurements according to ISO 20906). The average time difference between these two monitors (about 90 s) can be attributed to the time it took an aircraft to move

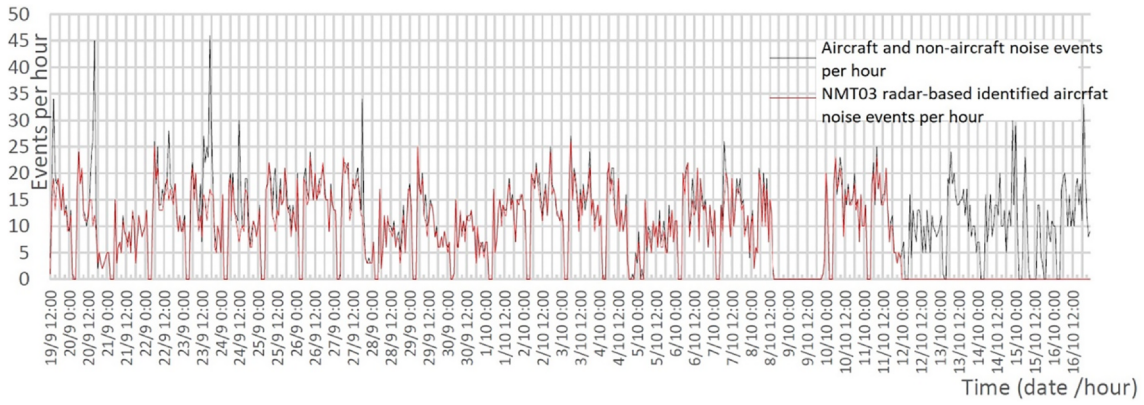

Fig. 5. Noise and aircraft events rate.

from its start point of the takeoff run to point 2 in Fig. 4 (the ADSB monitor location), where maximal noise was recorded. It can also be attributed to the fact that tower time of takeoff corresponds to takeoff clearance, rounded to the minute in the IAA publication.

When the aircraft noise was measured at its maximum (L_{ASmax}), the average ground distance between the aircraft and the ADSB monitor location (point 2 in Fig. 4) was about 415 m, and the average direction of the aircraft was 2100 to the ADSB monitor, relative to the north (i.e., south-southwest to the monitor). At that time, the average altitude of the aircraft was about 660 m, which means a slant distance of 780 m between the aircraft *location* and the ADSB monitor. However, the slant distance between the ADSB monitor and the aircraft *paths* is 620 m (Table 1). Therefore, there is a sound delay of almost 2 s, in which the aircraft moves almost 200 m due to its average climbing speed (about 100 m/s), which explains the 160 m difference between the two slant distances (the aircraft *location* and its *path*). This difference can also be attributed to the noise pattern of an aircraft (more noise behind the aircraft than on its sides).

The main result from comparing aircraft noise identification between the ADSB system and the NMT03 is that the ADS-B-driven system is at least as good as the radar-driven NMT03, as can be seen from Table 2.

The NMT03 monitor did not list seven aircraft noise events in the IAA data, which included Boeing 747–400 that caused a noise level of 86.8dBA, Boeing 757–200 with 77.6dBA, Boeing 737–800 with 81.2dBA, and Airbus 321 with a 76.8dBA noise level. These omissions in the IAA data can be a result of a failure in the radar, in the NMT03 monitor, or the data recording, analyzing, or reporting system. On the other hand, the ADS-B receiver did not detect five aircraft; two were small private jets that caused a noise level of 72–77dBA, two small-range ATR turboprops with a 70dBA, and one Boeing 737–400 with a 78.9dBA noise level. These omissions can be a result of inoperative or missing ADS-B equipment in those aircraft, GPS disturbances, or too narrow “square of interest”, as these aircraft might turn immediately after takeoff and exit the expected flight path. The NMT03 recorded 111 aircraft takeoffs from runway 26 during these 10 time-intervals (94% of all aircraft), whereas the ADSB system recorded 112 aircraft during the same time intervals (95% of all aircraft, and more than the NMT03 identifications). It should be noted, however, that on average, NMT03 detects just 85.5% of the aircraft, according to IAA (CAA IL, 2018).

One noise event, listed in Table 2 at 05:48, was recorded by the ADSB monitor, but has no match in the ADS-B data or the IAA’s NMT03 monitor data, and seems to be an aircraft noise according to its noise pattern, as shown in Fig. 7. Thus, out of the 121 aircraft noise events, just one seems to be missed by the suggested methodology as well as by the IAA system, i.e., the NMT03 monitor, probably a special flight or aircraft (non-commercial or non-civil).

Noise measurements in those ten hours, spread over several parts of the day as described above, along with ADS-B triggers for aircraft presence, are shown in Figs. 6 and 7. Aircraft noise is clearly identified in the recorded noise, without the need to analyze the sound pattern or use any other means to recognize it. Even in times of substantial background noise events, or aircraft noises that originated in other places (e.g., from other runways, or crossing above), clear identification of relevant aircraft noise is achieved. This is shown, for example, in Fig. 7, around 10:30 AM, when a correct aircraft noise identification was achieved, despite substantial background noise, with some of the events resembling aircraft noise.

Although the ADS-B triggers are not precisely aligned with the 10dBA down period, it can easily be identified, using L_{ASmax} in the triggered interval, and looking for the 10dBA down points before and after the time of L_{ASmax} recoding.

The suggested methodology is ISO 20906 compliant and provides better identification results than those required by ISO 20906 in its section 4.5 (aircraft sound event detection and classification). ISO 20906 requires that more than 50% of the true number of aircraft noise events are identified correctly (true positive), while the number of non-aircraft noise events, which are incorrectly identified as aircraft noise events (false positive), is less than 50% of the true number of aircraft noise events. The results of the experiments in 10 intervals with the ADS-B system indicated a true positive of about 95% (better than the radar-driven NMT03 monitor) and 0% false positive or false negative during these specific intervals when both systems (ADSB and NMT03) were tested simultaneously.

Table 2
Noise measurements, ADSB and IAA data.

Date	ADSB data							IAA data			
	Time	**ICAO24**	**Latitude**	**Longitude**	**Altitude**	**type**	**L_{ASmax}**	**Time**	**Flight**	**type**	**L_{ASmax}**
24/12/2019	0:12:20	AB4C1D	32.00650	34.82620	1804	A333	82.7	0:11:00	DAL469	A333	87.9
	0:21:47	738,072	32.00562	34.82273	1725	B772	83.7	0:20:00	ELY025	B772	82.9
	0:25:14	4B84E7	32.00363	34.81315	2650	A321	77.3	0:24:00	KKK6221	A321	76.2
	0:27:03	7380C7	32.00556	34.82355	1583	B789	79.6	0:26:00	ELY001	B789	78.6
	0:58:15	740,822	32.00600	34.82719	2000	B788	74.3	0:57:00	RJA341	B787	74.1
	5:03:15	451E90	32.00594	34.82397	2225	A320	75.6	5:02:00	LZB572	A320	74.7
	5:05:01	4841A6	32.00528	34.82111	1800	B739	83.1	5:04:00	KLM462	B739	82.6
	5:09:23	3C6488	32.00369	34.81438	2712	A321	76.6	5:08:00	DLH691	A321	79.1
	5:15:08	3004C2	32.00429	34.81729	2247	B738	81.2	Not recorded			
	5:17:08	4BA9C2	32.00546	34.82238	2700	A332	78.9	5:16:00	THY793	A332	78.1
	5:19:18	738,052	32.00073	34.75167	3061	B739	83.6	5:18:00	ELY311	B739	84.0
	5:21:19	4B1880	32.00450	34.82089	2125	A333	79.8	5:20:00	SWR257	A333	81.7
	5:23:42	4BB855	32.00560	34.82474	2425	A20N	70.6	5:22:00	PGT786	A320	71.7
	5:25:25	300,068	32.00476	34.82077	2225	A321	78.5	5:23:00	AZA809	A321	80.0
	5:27:52	Not detected					78.9	5:26:00	LOT152	B734	77.6
	5:29:49	3444CC	32.00508	34.82061	2325	A320	76.2	5:28:00	VLG7845	A320	76.9
	5:33:21	495,301	32.00511	34.82310	1725	A21N	75.9	5:32:00	TAP1604	A21N	74.3
	5:35:12	4692D6	32.00527	34.82263	2625	A320	72.6	5:33:00	AEE563	A320	71.4
	5:37:41	4690F0	32.00425	34.81743	2467	A321	77.2	5:37:00	AEE929	A321	77.1
	5:39:38	738,064	32.00585	34.82340	1756	B738	81.9	5:38:00	ELY321	B738	81.5
	5:43:47	Not detected					72.1	5:42:00	3414XCOZ	C550	71.1
	5:52:18	501D1E	32.00560	34.82198	2075	A319	78.4	5:51:00	CTN357	A319	77.1
	5:56:12	49D38C	32.00537	34.82136	1594	B739	81.4	5:55:00	TVS1287	B739	80.5
	10:00:12	4BA9D4	32.00542	34.82358	1825	A333	82.6	9:59:00	THY785	A333	83.1
	10:10:27	Takeoff from runway 30					68.9	10:09:00	AIZ2821	A21N	65.9
	10:14:03	47340A	32.00469	34.82020	2347	A320	75.5	10:13:00	WZZ4428	A320	73.2
	10:15:50	501E3C	32.00443	34.82020	2625	A320	74.2	10:15:00	ISR713	A320	77.6
	10:17:44	040,077	32.00423	34.82051	1875	B738	81.4	10:17:00	ETH415	B738	79.6
	10:21:28	Not detected					77.1	10:20:00	1404XCZA	C650	77.0
	10:28:49	471EA8	32.00540	34.82154	2200	A320	75.9	10:27:00	WZZ3258	A320	73.1
	10:31:32	471F55	32.00522	34.82150	2140	A320	76.2	10:29:00	WZZ3808	A320	74.2
	10:44:12	738,284	32.00583	34.82655	2125	A320	75.1	10:43:00	ISR885	A320	73.9
	10:48:12	Not detected					70.4	10:46:00	ISR587	AT72	69.0
	10:53:40	471F91	32.00548	34.82064	1845	A320	77.6	10:52:00	WZZ3480	A320	75.9
	10:56:14	7380C4	32.00560	34.82353	1700	B789	80.7	10:55:00	ELY007	B789	79.3
	10:58:47	473,410	32.00578	34.82073	2125	A320	76.4	10:58:00	WZZ3594	A320	75.3
	16:03:19	738,287	32.00508	34.82038	2297	A320	76.0	16:02:00	ISR573	A320	75.4
	16:06:26	73806A	32.00466	34.82072	2275	B738	80.4	16:05:00	ELY333	B738	79.8
	16:08:08	Not detected					69.7	16:07:00	ISR439	AT72	66.8
	16:11:15	3004C2	32.00601	34.82478	1814	B738	80.7	16:10:00	NOS9071	B738	80.8
	16:15:17	73806C	32.00429	34.81701	2327	B738	78.1	16:14:00	ELY363	B738	79.0
	16:18:20	34558F	32.00570	34.82289	1750	B789	76.6	16:17:00	AEA1302	B789	75.1
	16:21:49	4B1885	32.00599	34.82712	1680	A333	83.0	16:21:00	SWR253	A333	81.9
	16:27:21	43EA1C	32.00386	34.81914	2906	CL60	66.7	Not recorded			
	16:29:26	738,064	32.00587	34.82432	1872	B738	80.6	16:28:00	ELY339	B738	81.1
	16:35:03	4BB84D	32.00465	34.82066	2650	A20N	72.4	16:34:00	PGT784	A320	72.0
	16:36:49	738,060	32.00513	34.82184	2250	B738	79.1	16:36:00	ELY2431	B738	77.4
	16:38:43	44CDC5	32.00463	34.82005	2125	A320	77.6	16:37:00	BEL3290	A320	78.7
	16:42:48	424B04	32.00446	34.81974	2125	GLEX	72.1	16:43:00	QASMAGMA	GLEX	67.3
	16:44:49	43E84A	32.00353	34.81563	2851	E35L	66.7	16:44:00	LAUMBIRD	E35L	65.6
	16:48:46	440C8C	32.00682	34.83207	1625	A321	72.4	16:48:00	AUA858	A321	76.6
	16:54:32	7380C9	32.00471	34.82010	1750	B789	79.8	16:53:00	ELY011	B789	79.3
	16:57:08	3C706B	32.00562	34.82324	2725	MD11	80.8	16:55:00	DLH8343	MD11	79.5
	16:59:33	738,065	32.00423	34.81936	2471	B738	77.9	16:58:00	ELY5181	B738	80.0
	20:07:46	AC7AD2	32.00354	34.81586	2625	B752	77.6	Not recorded			
	20:10:32	Takeoff from runway 30					72.2	20:09:00	AIZ1805	E195	70.9
	20:14:23	300,069	32.00463	34.82009	2621	A321	75.7	20:13:00	AZA822	A321	75.6
	20:20:51	4BAA46	32.00433	34.81790	2110	A321	79.0	20:19:00	THY837	A321	77.6
	20:24:43	4691C4	32.00400	34.81562	2575	A320	74.4	20:23:00	AEE925	A320	73.4
	20:35:05	3C70B5	32.00317	34.81472	3325	B752	71.8	20:33:00	BCS961	B757	71.8
	20:48:50	471F7A	32.00466	34.81635	2425	A321	77.5	20:47:00	WZZ1560	A321	76.7
	20:52:25	505CD8	32.00578	34.82150	1725	B738	79.9	20:51:00	ELY5147	B738	79.5
	20:58:31	738C06	32.00448	34.81821	1875	B744	86.8	Not recorded			

(*continued on next page*)

Table 2 (*continued*)

Date	ADSB data							IAA data			
	Time	**ICAO24**	**Latitude**	**Longitude**	**Altitude**	**type**	**L_{ASmax}**	**Time**	**Flight**	**type**	**L_{ASmax}**
26/9/2019	00:06:29	508,395	32.00355	34.81377	2150	B738	80.4	00:05:00	AUI772	B738	79.8
	00:09:23	AB4FD4	32.00512	34.82111	1931	A333	89.0	00:08:00	DAL469	A333	88.1
	00:13:00	4B8DEE	32.00500	34.82323	2000	B738	77.8	00:12:00	CAI446	B738	77.4
	00:15:55	A1C7E4	32.00545	34.81887	1800	B77W	87.6	00:14:00	UAL091	B773	86.5
	00:31:23	4B8685	32.00552	34.82252	2256	A321	76.4	00:30:00	KKK6221	A321	77.2
	00:39:10	7380C7	32.00536	34.82223	1700	B789	80.4	00:37:00	ELY001	B789	79.2
	00:45:49	740,822	32.00466	34.82072	2200	B788	75.5	00:44:00	RJA341	B787	73.2
	00:51:03	738,072	32.00592	34.82380	1825	B772	83.8	00:50:00	ELY025	B772	83.7
	00:53:55	5083CD	32.00533	34.82364	1975	B738	78.7	00:52:00	AUI2304	B738	78.3
	5:02:14	501D1F	32.00532	34.81955	2192	A320	78.0	05:00:00	CTN3057	A320	77.0
	5:03:54	738,488	32.00513	34.82117	1750	E195	79.9	05:02:00	AIZ413	E195	79.4
	5:07:30	48418B	32.00553	34.82415	1725	B739	83.0	05:06:00	KLM462	B739	81.8
	5:11:18	44CDCB	32.00624	34.82070	2198	A320	77.2	05:10:00	BEL3294	A320	77.9
	5:13:45	505CD8	32.00653	34.82318	1250	B738	84.5	05:12:00	ELY5425	B738	84.6
	5:16:39	3C648D	32.00378	34.81541	2725	A321	75.9	05:15:00	DLH691	A321	75.1
	5:19:47	738,052	32.00478	34.82079	2073	B739	81.4	05:18:00	ELY311	B739	82.2
	5:23:03	4B187D	32.00446	34.81971	2025	A333	82.9	05:21:00	SWR257	A333	81.8
	5:26:27	49D38C	32.00547	34.82109	1700	B739	81.1	05:25:00	TVS1287	B739	80.5
	5:30:57	495,301	32.00527	34.82207	2050	A21N	76.9	05:29:00	TAP1604	A21N	76.4
	5:34:36	4690F4	32.00486	34.81976	2400	A321	76.8	05:33:00	AEE929	A321	75.4
	5:37:47	300,067	32.00461	34.82018	2250	A321	78.2	05:36:00	AZA809	A321	79.2
	5:40:40	73806A	32.00430	34.82062	2057	B738	80.2	05:39:00	ELY321	B738	80.2
	5:42:24	4BB1E6	32.00462	34.81915	2000	A333	81.8	05:41:00	THY793	A333	80.1
	5:45:03	4BB865	32.00532	34.82302	2725	A20N	71.6	05:43:00	PGT786	A20N	71.4
	5:46:50	738,284	32.00472	34.82065	2434	A320	74.6	05:45:00	ISR835	A320	73.1
	5:48:30	Undetected					74.5	Not recorded			
	5:51:32	4692D6	32.00513	34.82122	2574	A320	73.8	05:50:00	AEE563	A320	72.6
	5:57:59	3001C5	32.00559	34.82235	1900	B738	81.8	05:56:00	NOS3235	B738	82.0
29/9/2013	10:00:25	4D21E6	32.00561	34.82108	2023	B738	77.5	09:59:00	BBG752	B738	76.3
	10:03:54	4BA9CA	32.00477	34.81857	2428	A333	80.5	10:02:00	THY785	A333	80.4
	10:11:02	451E90	32.00607	34.82390	2125	A320	75.9	10:09:00	LZB6618	A320	76.1
	10:17:41	04003B	32.00545	34.82139	1700	B738	82.1	10:16:00	ETH415	B738	80.6
	10:20:39	471F4A	32.00479	34.82114	2766	A320	74.4	10:19:00	WZZ4428	A320	72.8
	10:25:56	7380C0	32.00609	34.82214	1650	B789	77.6	10:24:00	ELY315	B789	77.4
	10:29:48	738,286	32.00514	34.82187	2215	A320	76.1	10:31:00	ISR343	A320	77.1
	10:34:58	4D216D	31.99533	34.82929	2025	B733	82.6	10:33:00	BBG442	B733	81.5
	10:40:03	Takeoff from runway 30					70.1	10:38:00	ISR429	AT72	69.2
	10:46:22	4CA852	32.00480	34.82151	2425	B738	76.3	10:45:00	RYR2824	B738	74.7
	10:49:02	43EA1C	32.00530	34.82507	2850	CL60	66.5	Not recorded			
	10:54:57	47340D	32.00581	34.82491	2200	A320	76.0	10:53:00	WZZ3258	A320	75.4
	10:57:26	4690F3	32.00601	34.82507	2325	A321	76.8	Not recorded			
	11:00:14	4B8E46	32.00384	34.81600	2444	B738	78.5	10:59:00	PGT796	B737	79.9
	16:05:34	4B187D	32.00568	34.82454	1927	A333	81.5	16:05:00	SWR253	A333	81.3
	16:14:35	44CDCE	32.00630	34.82596	2109	A320	77.8	16:13:00	BEL3290	A320	78.9
	16:20:00	440C8C	32.00569	34.82512	1875	A321	77.9	16:19:00	AUA858	A321	76.7
	16:22:49	346,181	32.00652	34.82803	1525	B789	78.3	16:21:00	AEA1302	B789	76.1
	16:26:25	4BD183	32.00210	34.82100	2475	B734	79.0	16:25:00	TWI504	B734	77.8
	16:28:25	4B8E13	32.00478	34.82023	2500	B738	78.9	16:27:00	PGT784	B738	79.0
	16:43:26	738,485	32.00472	34.82136	2343	E190	76.8	16:41:00	AIZ1819	E195	75.5
	16:48:35	3C666C	32.00611	34.82901	2550	A321	74.7	16:47:00	DLH687	A321	75.0
	20:08:35	3964F3	32.00409	34.81661	2050	B738	80.2	20:07:00	TVF4741	B738	80.7
	20:15:46	4CA8FF	32.00519	34.82223	2323	A320	75.8	20:15:00	AZA822	A320	75.3
	20:17:30	471EFC	32.00392	34.81646	2350	A321	78.6	20:16:00	WZZ1560	A321	76.2
	20:25:26	440,051	32.00448	34.81836	2375	A320	75.4	20:26:00	EJU3738	A320	75.0
	20:30:10	5083C9	32.00467	34.82145	1883	B738	78.2	20:28:00	AUI782	B738	77.6
	20:32:06	4690FA	32.00545	34.82352	2317	A320	75.2	20:31:00	AEE925	A320	72.6
	20:47:09	E80200	32.00601	34.82377	1429	B788	80.4	20:46:00	LAN713	B787	79.6
	20:50:19	A5D4C3	32.00410	34.81921	2728	B744	80.3	20:49:00	GTI603	B744	77.7

5. Conclusions

Currently, synchronization of sound level measurements with the airport's surveillance radar is the most commonly used methodology for identifying aircraft noise and separating it from background noise. It is simple and accurate, but it can only be applied near airports equipped with surveillance radar, by airport authorities, or with their cooperation in providing the radar tracings data.

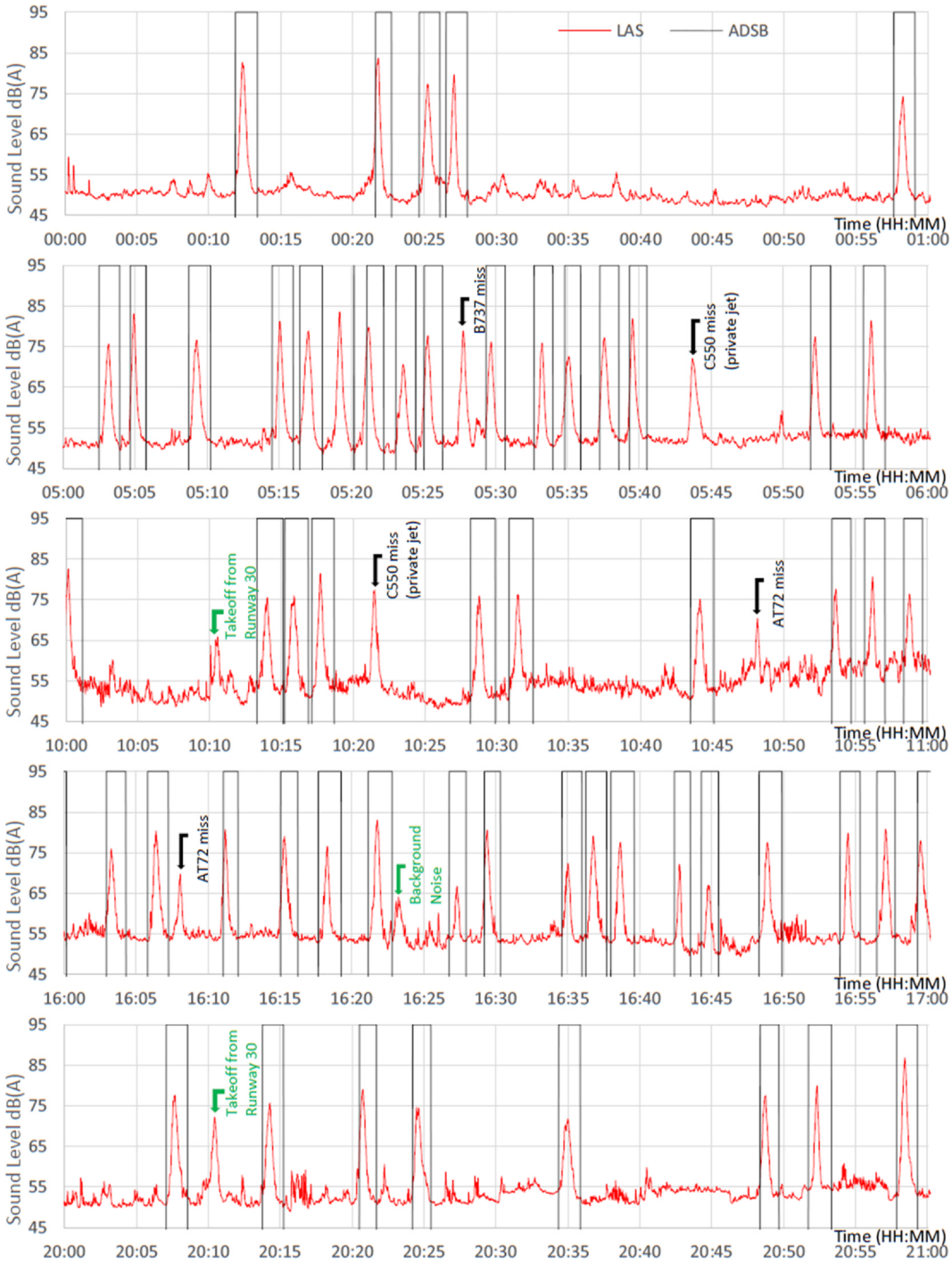

Fig. 6. Noise and ADS-B triggers 24/9/2019.

ADS-B signals are transmitted practically by almost every aircraft that might be a subject of noise measurement, i.e., commercial aircraft taking-off or landing in airports that are close to urban centers. Moreover, USA and European legislation mandate ADS-B in these aircraft by 2020. These signals can be received by simple and inexpensive receivers, can be decoded, and can provide triggers and valuable information to unattended noise monitors (and to the attended one as well), e.g., location, altitude, speed and direction of the aircraft, its identity and type, and more. This information can be used to significantly enhance the ability to discriminate aircraft noise by defining the exact time and place of the noise source. These conclusions were demonstrated experimentally, and compared with an unattended remote sound monitor, driven by an airport surveillance radar.

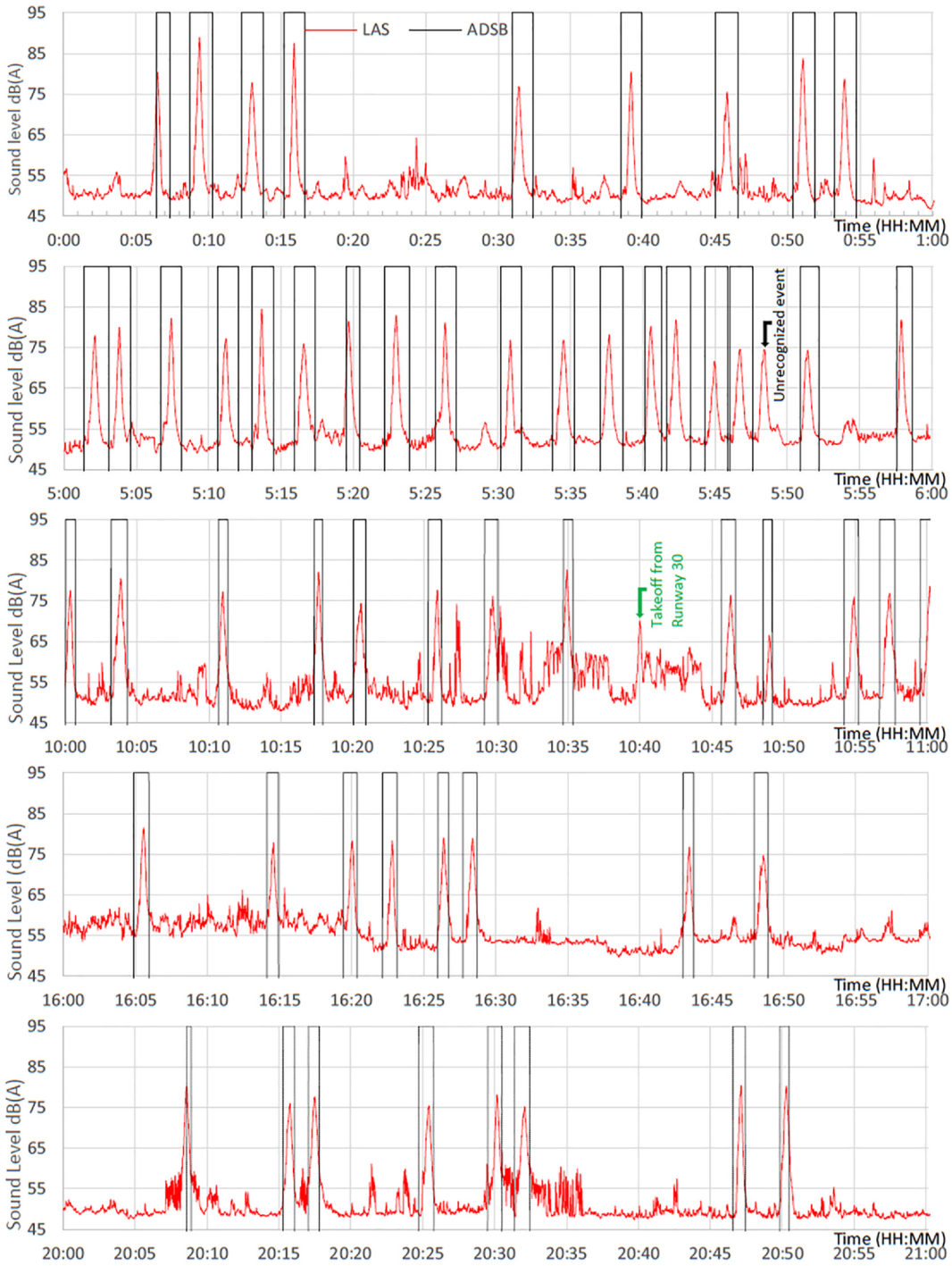

Fig. 7. Noise and ADS-B triggers 26/9/2019 & 29/9/2019.

We showed that ADS-B is at least as accurate as the airport's surveillance radar, while independent of airport permission and cooperation in conducting aircraft noise surveillance. Hence this methodology can be used by non-airport entities or administrations, e.g., communities, researches, or environmental organizations. Furthermore, this methodology can also be used to enhance the accuracy of noise measurements in small airports lacking surveillance radar.

The suggested methodology can also be used along with other means of aircraft noise surveillance methods, such as the directivity. Usage of ADS-B signals can trigger a microphone array (as in (Merino-Martinez et al., 2016b; Snellen et al., 2017)) and improve the "beamforming" by indicating the measured aircraft, its location, speed, direction, and flight path. Adding the directivity

methodology to the ADS–B methodology can improve the discrimination of aircraft noise from simultaneous background noise, and can help to ignore other sources of noise in cases of quiet aircraft.

Acknowledgments

Thanks to Omer Pony for his assistance in programming and measurements, Osnat Arnon from TOP Environment & Acoustics, and Yair Liel for their valuable ideas and comments.

References

Asensio, C., Pavón, I., Ruiz, M., Pagan, R., Recuero, M., 2007. Estimation of directivity and sound power levels emitted by aircrafts during taxiing, for outdoor noise prediction purpose. Applied Acoustics 68 (10), 1263–1279.
Asensio, C., Ruiz, M., Recuero, M., 2010. Real-time aircraft noise likeness detector. Applied Acoustics 71 (6), 539–545.
Asensio, C., Recuero, M., Ruiz, M., 2012. Aircraft noise-monitoring according to ISO 20906. Evaluation of uncertainty derived from the classification and identification of aircraft noise events. Applied Acoustics 73 (3), 209–217.
Asensio, C., Ruiz, M., Recuero, M., Moschioni, G. and Tarabini, M., 2015. "A novel intelligent instrument for the detection and monitoring of thrust reverse noise at airports", Acta IMEKO, vol. 4, no. 1, article 3, pp. 5-10.
Civil Aviation Authority (UK), 2016. "Aircraft Noise and Health Effects: Recent Findings", CAP1278.
EU Directive 2002/30, 2002. "Establishment of rules and procedures with regard to the introduction of noise-related operating restrictions at community airports".
EU Regulation 598/2014, 2014. "Establishment of rules and procedures with regard to the introduction of noise-related operating restrictions at Union airports within a Balanced Approach".
EU Commission Implementing Regulation 1207/2011, "Laying down requirements for the performance and the interoperability of surveillance for the single European sky", 2011.
EU Commission Implementing Regulation 2020/587, 2020. "Amending Implementing Regulation (EU) No 1207/2011 and Implementing Regulation (EU) No 1206/2011".
European Civil Aviation Conference (ECAC) Doc 29, 2016. "Report on Standard Method of Computing Noise Contours around Civil Airports", 4th edition, Vol. 2.
Federal Aviation Administration, Aviation Environmental Design Tool (AEDT), 2020. "Technical Manual", Version 2d, 2017, and "User Manual", Version 3c.
Fidell, S., Schomer, P., 2007. Uncertainties in measuring aircraft noise and predicting community response to it. Noise Control Engineering Journal 55 (1), 82–88.
Filippone, A., Zhang, M., Bojdo, N., 2019. Validation of an integrated simulation model for aircraft noise and engine emissions. Aerospace Science and Technology 89, 370–381.
Gagliardi, P., Fredianelli, L., Simonetti, D., Licitra, G., 2017. ADS-B system as a useful tool for testing and redrawing noise management strategies at Pisa airport. Acta Acustica united Acustica 103 (4), 543–551.
Gagliardi, P., Teti, L., Licitra, G., 2018. A statistical evaluation on flight operational characteristics affecting aircraft noise during take-off. Appl. Acoustics 134, 8–15.
Genescà, M., Romeu, J., Pàmies, T., Sánchez, A., 2009. Real time aircraft fly-over noise discrimination. J. Sound Vibration 323, 112–129.
Genescà, M., Romeu, J., Pàmies, T., Sánchez, A., 2010. Aircraft noise monitoring with linear microphone arrays. IEEE Aerospace Electronic Systems Magazine 25 (1), 14–18.
Genescà, M., Romeu, J., Arcos, R., Martín, S., 2013. Measurement of aircraft noise in a high background noise environment using a microphone array. Transportation Research Part D: Transport and Environment 18, 70–77.
Genescà, M., 2016. Directional monitoring terminal for aircraft noise. J. Sound Vibration 374, 77–91.
International Civil Aviation Organization (ICAO), 2018. "ICAO Long-Term Traffic Forecasts", https://www.icao.int/sustainability/Documents/LTF_Charts-Results_2018edition.pdf.
International Civil Aviation Organization (ICAO), Environmental Technical Manual, Volume I. Procedures for the Noise Certification of Aircraft, Doc 9501, AN/929, 2nd ed., 2015.
International Civil Aviation Organization (ICAO), 2008. "The balanced approach", Doc 9829, 2nd ed..
International Civil Aviation Organization (ICAO) Annex 16 – Environmental Protection – Vol I – Aircraft Noise, 2017. 8th ed..
International Civil Aviation Organization (ICAO) ADS-B Implementation and operations guidance document, 2018. 11th ed..
International Civil Aviation Organization (ICAO) Technical Provisions for Mode S Services and Extended Squitter, 2012. Doc 9871, 2nd ed..
International Civil Aviation Organization (ICAO), 2018. "Recommended Method for Computing Noise Contours around Airports", Doc. 9911, 2nd ed..
ISO 20906:2009, 2009. "Acoustics – Unattended monitoring of aircraft sound in the vicinity of airports".
Israel Airport Authority (IAA), 2019. Monthly Noise Reports, https://www.iaa.gov.il/he-IL/natureandenvironment/pages/NoiseMonitoringMonthlyReport.aspx.
Israel Airport Authority (IAA), 2020. "Calibrating Ben-Gurion airport's noise monitoring system compared to 2018 AEDTs", in General / Other Appendix - Data for making a noise map for 2018, http://www.mavat.moin.gov.il/MavatPS/.
Merino-Martinez, R., Bertsch, L., Snellen, M., Simons, D.G., 2016a. Analysis of landing gear noise during approach. Proc Of the 22nd AIAA/CEAS Aeroacoustics Conference. https://doi.org/10.2514/6/2016-2769.
Merino-Martinez, R., Heblij, S.J., Bergmans, D.H.T., Snellen, M., Simons, D.G., 2019. Improving aircraft noise predictions considering fan rotational speed. J. Aircraft 56 (1), 284–294. https://doi.org/10.2514/1.C034849.
Merino-Martínez, R., Luesutthiviboon, S., Zamponi, R., Rubio Carpio, A., Ragni, D., Sijtsma, P., Snellen, M., Schram, C., 2020. Assessment of the accuracy of microphone array methods for aeroacoustic measurements. J. Sound Vibration 470.
Merino-Martinez, R., Snellen, M., Simons, D.G., 2016b. Functional beamforming applied to imaging of flyover noise on landing aircraft. Journal of Aircraft 53 (6), 1830–1843. https://doi.org/10.2514/1.C033691.
Maijala, P., Shuyang, Z., Heittola, T., Virtanen, T., 2018. Environmental noise monitoring using source classification in sensors. Applied Acoustics 129, 258–267.
Pak, J.W. and Kim, M.K., 2019. "Convolutional Neural Network Approach for Aircraft Noise Detection", in Proc. of the 1st International Conference on Artificial Intelligence in Information and Communication (ICAIIC 2019), pp. 430-434.
Rodríguez-Díaz, A., Adenso-Díaz, B., González-Torre, P.L., 2017. A review of the impact of noise restrictions at airports. Transportation Research Part D: Transport and Environment 50, 144–153.
Sánchez-Pérez, L.A., Sánchez-Fernández, L.P., Suárez-Guerra, S., Carbajal-Hernández, J.J., 2013. Aircraft class identification based on take-off noise signal segmentation in time. Expert Systems with Applications 40, 5148–5159.
Sánchez-Pérez, L.A., Sánchez-Fernández, L.P., Suárez-Guerra, S., Márquez-Molina, M., 2014. Geo-referenced flight path estimation based on spatio-temporal information extracted from aircraft take-off noise. Digital Signal Processing 30, 1–14.
Sanfilippo, S., 2012. "Dump1090 is a simple Mode S decoder for RTLSDR devices", https://github.com/antirez/dump1090.
Snellen, M., Merino-Martinez, R., Simons, D.G., 2017. Assessment of noise level variability on landing aircraft using a phased microphone array. J. Aircraft 54, 2173. https://doi.org/10.2514/1.C033950.
Sun, J., Vû, H., Hoekstra, J., EllerBroek, J., 2020. The 1090MHz Riddle. https://mode-s.org/decode/index.html.
Tarabini, M., Moschioni, G., Asensio, C., Bianchi, D., Saggin, B., 2014. Unattended acoustic events classification at the vicinity of airports. Applied Acoustics 84, 91–98.
Taylor, D., 2019. "ADS-B using dump1090 for the Raspberry Pi", https://www.satsignal.eu/raspberry-pi/dump1090.html.
Torija, A.J., Self, R.H., 2018. Aircraft classification for efficient modelling of environmental noise impact of aviation. J. Air Transport Management 67, 157–168.
US "Airport Noise and Capacity Act of 1990 ("ANCA")", 1990. 49 U.S.C., Chapter 475.
US Code of Federal Regulations: 14 CFR §91.225, 2019. "Automatic Dependent Surveillance-Broadcast (ADS-B) Out equipment and use", Amdt. 91-355, 84 FR 34287.
Zellmann, C., Schäffer, B., Wunderli, J.M., Isermann, U., Paschereit, C.O., 2017. Aircraft noise emission model accounting for aircraft flight parameters. J. Aircraft. https://doi.org/10.2514/1.C034275.
Zhang, F., Graham, D.J., 2020. Air transport and economic growth: a review of the impact mechanism and causal relationships. Transp. Rev. https://doi.org/10.1080/01441647.2020.1738587.
Zhang, J., Liu, W., Zhu, Y., 2011. Study of ADS-B Data Evaluation. Chinese J. Aeronautics 24 (4), 461–466.